Available online at www.sciencedirect.com
SCIENCE DIRECT®
International Journal of Pharmaceutics 286 (2004) 131–145
international journal of pharmaceutics
www.elsevier.com/locate/ijpharm

Pharmaceutical Nanotechnology

Improved photodynamic activity of porphyrin loaded into nanoparticles: an in vivo evaluation using chick embryos

Angelica Vargas[a], Bernadette Pegaz[b], Elodie Debefve[b], Yvette Konan-Kouakou[b], Norbert Lange[a], Jean-Pierre Ballini[b], Hubert van den Bergh[b], Robert Gurny[a], Florence Delie[a,*]

[a] *Department of Pharmaceutics and Biopharmaceutics, School of Pharmacy, University of Geneva, 30, quai E. Ansermet, CH-1211 Geneva 4, Switzerland*
[b] *Institute of Environmental Engineering, Swiss Federal Institute of Technology, Lausanne, Switzerland*

Received 1 April 2004; received in revised form 23 July 2004; accepted 30 July 2004
Available online 29 September 2004

Abstract

Hydrophobic porphyrins are potentially interesting molecules for the photodynamic therapy (PDT) of solid cancers or ocular vascularization diseases. Their pharmaceutical development is, however, hampered by their lipophilicity, which renders formulation difficult especially when intravenous administration is needed. Encapsulation of a lipophilic derivative of porphyrin, the meso-tetra(*p*-hydroxyphenyl)porphyrin (*p*-THPP), into polymeric biodegradable poly(D,L-lactide-*co*-glycolide) (PLGA) nanoparticles proved to enhance its photodynamic activity against mammary tumour cells when compared to free drug. In order to further investigate these carriers, the efficacy of the encapsulated drug was assessed on the chick embryo chorioallantoic membrane (CAM) model. First, we identified a suitable solvent for the drug in terms of *p*-THPP solubility and tolerability by chick embryos. This solution was used as a reference. Then, the fluorescence pharmacokinetics and the photodynamic effects of the porphyrin on CAM vessels were evaluated after intravenous administration of either a *p*-THPP solution (free drug) or the drug loaded into nanoparticles. The results showed that: (i) the drug remained longer in the vascular compartment when incorporated into nanoparticles and (ii) vascular effects of *p*-THPP after light irradiation were enhanced with nanoparticle carriers. These results are discussed taking into account the extravasation of intravascular circulating photosensitizers and its influence on PDT performance.

Keywords: Photodynamic therapy (PDT); Biodegradable nanoparticles; Chick chorioallantoic membrane (CAM) model; Drug delivery system; Porphyrin (*p*-THPP); Extravasation

* Corresponding author. Tel.: +41 22 379 65 73; fax: +41 22 379 65 67.
E-mail address: florence.delie@pharm.unige.ch (F. Delie).

0378-5173/$ – see front matter © 2004 Elsevier B.V. All rights reserved.
doi:10.1016/j.ijpharm.2004.07.029

1. Introduction

Photodynamic therapy (PDT) is based on the administration of a photosensitizing agent (also known as a photosensitizer, PS), which is further activated by external irradiation with light. This therapy results in a sequence of photochemical and photobiological processes that trigger irreversible damage to the irradiated tissues. The main therapeutic applications of PDT are cancer therapy (Dougherty et al., 1998) and the treatment of neovascularization-related disorders such as choroidal neovascularization (CNV) secondary to age-related macular degeneration (AMD), one of the leading causes of blindness in elderly people in Western countries (Ferris et al., 1984; Klein et al., 1992). Since photosensitizers are inactive without light activation, this treatment can be considered to be selective to the illuminated area and a decrease in adverse effects is expected especially in cancer treatment. Most photosensitizers are porphyrin-like macrocycles and include porphyrins, chlorins and bacteriochlorins (Sternberg et al., 1998). Hydrophobic porphyrins, such as benzoporphyrin derivative monoacid ring A (BPD-MA), are potentially interesting molecules for PDT either in the treatment of solid cancers or ocular vascularization diseases (Sharman et al., 1999; Schmidt-Erfurth and Hasan, 2000; Renno and Miller, 2001). Indeed, BPD-MA encapsulated into liposomes (Visudyne®) is the first PS approved for clinical PDT of classic subfoveal choroidal neovascularization. The development of hydrophobic photosensitizers is, however, hampered by formulation problems due to their lipophilicity especially when intravenous (IV) administration is needed. Different approaches have been proposed such as the incorporation of PS into liposomes, micelles, polymeric particles, and low density lipoproteins, and the development of hydrophilic polymer-drug complexes, as recently reviewed by Konan et al. (2002). Micellar systems can be regarded as suitable vehicles for hydrophobic PS. However, emulsifying agents used for their preparation, such as Cremophor-EL, have been reported to elicit acute hypersensitivity and anaphylactic reactions in vivo (Gelderblom et al., 2001). Different liposomal strategies have been developed to target PS to tumour tissues, as reviewed by Derycke and de Witte (2004). Although liposomal formulations can substantially improve both PDT efficacy and PS safety, conventional liposomes have limitations such as short shelf life and chemical and physical instability in biological environments. However, improvement of liposomal formulations has been reported with the design of liposomes with specifically modified moieties (Woodle, 1998; Drummond et al., 1999; Derycke and de Witte, 2004). Polymeric nanoparticles offer numerous advantages over the conventional drug delivery systems including high drug loading, controlled release, and a large variety of carrier materials and manufacturing processes (Leroux et al., 1996; Konan et al., 2002). Recently, a hydrophobic photosensitizer, meso-tetra(*p*-hydroxyphenyl)porphyrin (Fig. 1a), was incorporated into polymeric biodegradable nanoparticles (Konan et al., 2003a). This system proved to be more effective than free porphyrin in inhibiting in vitro mammary tumour cell growth following PDT.

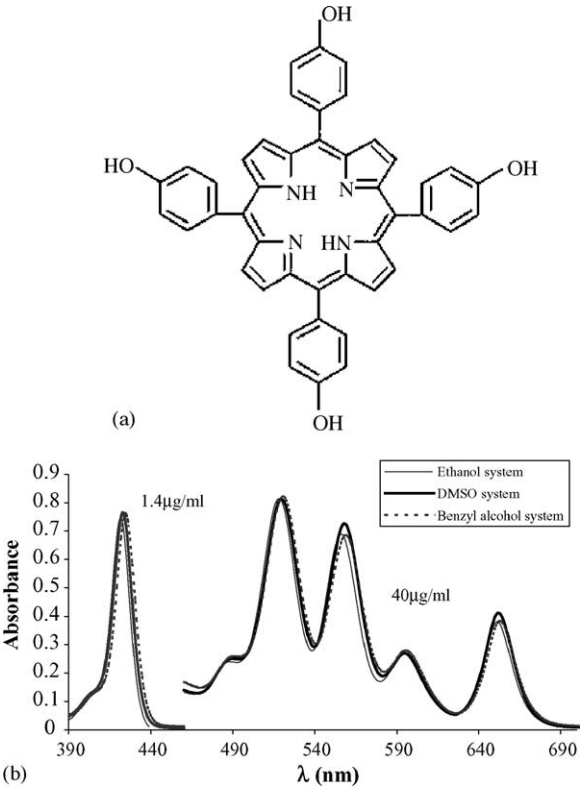

Fig. 1. Structural formula (a) and absorption spectra (b) of *p*-THPP dissolved in solvent systems containing 50% v/v of water, 30% v/v of PEG 400 and 20% v/v of either ethanol (—), DMSO (▬), or benzyl alcohol (- - -). *p*-THPP concentration: 1.4 μg/ml for λ = 390–460 nm and 40 μg/ml for λ = 461–700 nm.

The relatively low drug concentration and the short times of incubation of nanoparticles with cells required to induce satisfactory photodynamic damages demonstrated that *p*-THPP-loaded nanoparticles offer superior photoactivity compared to the free drug (Konan et al., 2003b). In order to further investigate these carriers, the efficacy of the encapsulated *p*-THPP was assessed in the chick chorioallantoic membrane (CAM) assay. The developing chicken embryo is surrounded by a chorioallantoic membrane, which becomes vascularized as the embryo develops. This in vivo model has been extensively used to study both angiogenesis and anti-angiogenesis (Ribatti et al., 2001). Moreover, the CAM model has been used to study the photothrombic effects of PDT after topical application of PS (Toledano et al., 1998; Hammer-Wilson et al., 1999), injection of PS into the yolk sac (Gottfried et al., 1995), intraperitoneal administration (Hornung et al., 1999), and intraamniotical injection (Peterka and Klepacek, 2001). Lange et al. (2001) demonstrated the feasibility of an IV administration of PS into CAM vessels. This approach allowed the CAM model to be used as a screening procedure for new PS intended for PDT of choroidal neovascularization (CNV). The distribution and the possible leakage from the vascular system of intravenously injected PS or fluorescent dyes in the CAM is followed by measuring the fluorescence of the vascularized and non-vascularized tissues; hence pharmacokinetic data can be obtained. Furthermore, the photodynamic activity of the PS can be assessed by evaluation of the vascular occlusion achieved after irradiation in a predefined area of the CAM. In this context, the CAM is a convenient model for monitoring the modifications of the vasculature. The transparency of its superficial layers allows an examination of structural changes of each blood vessel in real time. This in vivo model offers the advantage of being easily accessible, inexpensive and easy to handle (Lange et al., 2001). Furthermore, it is possible to use and compare different administration routes.

The objective of this work was to compare the vascular effects of *p*-THPP either as a free solution or encapsulated in polymeric nanoparticles on the CAM vessels. An aqueous solution was first developed and tested for its suitability as a reference. Then, the distribution and the photodynamic activity of the drug were compared when administered in both systems.

2. Materials

2.1. Chemicals

Poly(D,L-lactide-*co*-glycolide) (PLGA) with a copolymer ratio of 50:50 and molecular weight of 12 kDa (Resomer® RG502) was obtained from Boehringer Ingelheim (Ingelheim, Germany). Meso-tetra(*p*-hydroxyphenyl)porphyrin (*p*-THPP) was provided by Aldrich (Steinheim, Germany). Poly(vinyl alcohol) 87.7% hydrolyzed with a molecular weight of 26 kDa (Mowiol® 4-88), was obtained from Hoechst (Frankfurt/Main, Germany). D(+)-Trehalose dihydrate and phosphate buffered saline (PBS) were purchased from Sigma-Aldrich (Taufkirchen, Germany). Dimethyl sulfoxide (DMSO) was obtained from Acros Organics (New Jersey, USA). Polyethylenglycol 400 Ph Eur (PEG 400) was provided by Merck (Schuchardt, Germany). Sulforhodamine 101 was purchased from Lambda Physik (Göttingen, Germany). Ethanol 99.8%, benzyl alcohol, methylene blue and sodium chloride were obtained from Fluka (Buchs, Switzerland). All chemicals were of analytical grade and were used without further purification.

2.2. Microscope set-up

Fluorescence imaging of CAM vessels was performed with a CCD camera fitted to a fluorescence Eclipse 600 FN microscope equipped with an objective CFI achromat (magnification 4×, numerical aperture of 0.10 and working distance of 30 mm) (Nikon, Tokyo, Japan). Illumination was provided by a filtered 100-W mercury arc lamp. Light doses were measured with a calibrated 404 power meter (Spectra-Physics, Mountain View, CA). For the studies with *p*-THPP, the microscope was equipped with a fluorescence cube BV-2A (Nikon, Tokyo, Japan). This cube is composed of a 420 CWL filter, which provides excitation wavelengths between 400 and 440 nm, a dichroic mirror (455 nm), and a barrier filter (470 nm). An additional long path filter at 610 nm was added. For the fluorescence detection of sulforhodamine 101, a 11007WDGR cube (Chroma Technology Corp., Rockingham, VT, USA) was used. This cube is composed of a D535/50x filter, which provides excitation wavelengths between 510 and 560 nm, a dichroic mirror (565 nm), and a barrier filter (590 nm). Prior to injection of a fluorescent dye

or the photosensitizer, autofluorescence was recorded using the fluorescence cube BV-2A (Nikon, Tokyo, Japan) and an emission band pass filter D560/40m (Chroma Technology Corp., Rockingham, VT, USA).

3. Methods

3.1. Preparation and characterization of nanoparticles

p-THPP was encapsulated in PLGA 50:50 via the emulsification–diffusion technique as described by Konan et al. (2003a). Nanoparticles were purified by cross-flow filtration and freeze-dried in the presence of trehalose (trehalose: nanoparticle mass ratio of 2:1). The mean diameter of the freeze-dried nanoparticles, determined by photon correlation spectroscopy (Zetasizer 5000, Malvern, Worcesterhire, UK), was 117 ± 7 nm with a polydispersity index of 0.2 on a scale from 0 to 1. For the freeze-dried nanoparticles, a *p*-THPP loading of 7.8% (w/w) was determined spectrophotometrically with a Cintra 40 spectrometer (GBS, Victoria, Australia) at 653 nm as described by Konan et al. (2003a).

3.2. Formulation of a solution of p-THPP

For the preparation of *p*-THPP intended for IV administration, three formulations containing 50% v/v of water, 30% v/v of PEG 400 and 20% v/v of either ethanol, benzyl alcohol or DMSO were tested. These formulations are henceforward referred to as the ethanol, benzyl alcohol and DMSO systems, respectively. Absorption spectra of *p*-THPP in the different formulations were obtained with a Cintra 40 spectrometer (GBS, Victoria, Australia).

3.3. Chick chorioallantoic membrane (CAM) assay

The CAM assay was adapted from Lange et al. (2001) with the following modifications. All assays were done in triplicate, unless otherwise specified.

3.3.1. Egg incubation

Fertilized hen eggs (Animalerie universitaire, University of Geneva, Geneva, Switzerland) were placed into an incubator (Savimat MG 200, Chauffry, France) set at 37 °C and a relative humidity (RH) of 65%. Until embryo development day (EDD) 4, eggs were rotated twice a day. Then, a 3 mm hole was drilled in the eggshell at the narrow apex and was covered with adhesive tape. Eggs were then incubated without rotation until the CAM assay on EDD 12.

3.3.2. CAM preparation and injection procedure

On EDD 12, the hole in the eggshell was enlarged to a diameter of 2–3 cm allowing access to the CAM vasculature. Chick embryos were then placed under the objective of the fluorescence microscope. Formulations to be evaluated were injected into one of the principal blood vessels of CAM through a 33-gauge needle fitted to a 100 μl syringe (Hamilton, Reno, NV), enabling an assessment of (a) the tolerance to the formulations, (b) the pharmacokinetic parameters, (c) the influence of ethanol concentration on *p*-THPP extravasation, and (d) the photodynamic effect of *p*-THPP.

3.3.3. Embryo tolerance to solvents of p-THPP

Twenty, 50 or 100 μl of either ethanol system, benzyl alcohol system or DMSO system without *p*-THPP were injected. Methylene blue was dissolved in the systems (0.01% w/v) to allow visualization of the liquid during the injection. Survival rate of embryos was evaluated 24 h after IV administration ($n = 8$). Saline solution 0.9% w/v was used as a negative control.

3.3.4. Pharmacokinetic studies of p-THPP formulations

The residence time of *p*-THPP into CAM vessels was evaluated after IV administration of either *p*-THPP-loaded nanoparticles resuspended in PBS or *p*-THPP dissolved in the ethanol system. Time-dependent fluorescence angiographies were performed at different times during a period of 1500 s. Normalized photographic contrast (C_{phot}), as proposed by Lange et al. (2001) was used to express the evolution of the fluorescence intensity in blood vessels (I_{in}) in relation to the surrounding tissue (I_{out}).

$$C_{\text{phot}} = \frac{I_{\text{in}} - I_{\text{out}}}{(I_{\text{in}} + I_{\text{out}}) \times C_{\text{phot. max}}}$$

where $C_{\text{phot.max}}$ represents the highest photographic contrast obtained after administration.

3.3.5. Influence of ethanol concentration on p-THPP extravasation

Formulations containing 0.6 mg/ml of *p*-THPP and composed of 30% v/v of PEG 400, different concentrations of ethanol (either 15, 20, 30, 40 or 70% v/v) and water q.s. were prepared. An aliquot (10 μl) of a given formulation was injected into CAM vessels. Fluorescence angiographies were performed at 15, 30, 60, and 300 s after injection.

3.3.6. Photodynamic therapy and damage assessment

CAM was irradiated at 10, 15 or 20 J/cm^2 at 420 nm one minute after IV administration of *p*-THPP either loaded in nanoparticles or dissolved in the ethanol system. *p*-THPP doses were 0.3, 0.6, 1.2 and 2.5 mg per kg of chick embryo body weight, which in this study was estimated as 10 g according to Barnes and Jensen (1959), who determined the total tissue weight of chick embryos on EDD 12 as 9.71 ± 1.47 g (this value includes both embryo weight and extra embryonic membranes weight). The surface of the irradiated CAM area was 3 mm^2. Following PDT, the aperture in the shell was carefully covered with a plastic film (Parafilm, Pechiney Plastic Packaging, Chicago, IL) and treated eggs were maintained in the dark for 24 h in the incubator (37 °C, 65% RH). Then, 10 μl of a solution of sulforhodamine 101 in NaCl 0.9% (0.5 mg/ml) were injected into chick embryos in order to document vascular effects of photodynamic treatment by a fluorescence angiography of the irradiated area. Comparison of vessel fluorescence before and after PDT allowed an evaluation of vessel damage using an arbitrary damage scale proposed by Lange et al. (2001) presented in Table 1.

4. Results

4.1. Development of an injectable soluble formulation for p-THPP

In order to compare the nanoparticles to a reference, it was necessary to develop a suitable formulation for IV injection of *p*-THPP, a highly hydrophobic photosensitizer. Various solvent systems containing 20% v/v of an organic solvent (either ethanol, benzyl alcohol or DMSO), 30% v/v of PEG 400 and 50% v/v of water were tested. *p*-THPP was soluble in all systems at concentrations up to 2.5 mg/ml. The absorption spectra of *p*-THPP formulations show all the characteristic bands of porphyrins, and only minor differences between the three formulations are observed (Fig. 1b).

Since PDT effects on CAM vasculature are usually assessed 24 h after treatment, it is mandatory to evaluate the safety of *p*-THPP solvents towards chick embryos during that period. Survival rates of embryos were evaluated 24 h after administration of each formulation without *p*-THPP. The results are summarized in Fig. 2. By increasing injection volume, lower embryo survival rates were observed with all evaluated formulations, even with isotonic sodium chloride. The system containing benzyl alcohol appeared to be the most toxic: only 12.5% of embryos survived after injection of 20 μl of this formulation and the embryo death was observed immediately after injection of higher volumes. At 20 μl, the DMSO containing system was as innocuous as NaCl solution (0.9% w/v), however injection of higher volumes led to a decrease in survival rate to 62.5% for 50 μl and to 50% for 100 μl, respectively. The system containing ethanol was demonstrated to be as safe as aqueous NaCl solution at volumes of 20 μl

Table 1
Evaluation of PDT induced damage on CAM vessels

Damage scale*	Criterion
0	No damage
1	Partial closure of capillaries of diameter <10 μm
2	Closure of capillary system, partial closure of blood vessels of diameter <30 μm and size reduction of larger blood vessels
3	Closure of vessels of diameter <30 μm and partial closure of higher order vessels
4	Total closure of vessels of diameter <70 μm and partial closure of larger vessels
5	Total occlusion of vessels in the irradiated area

From Lange et al. (2001).

* Intermediate values are found when making the average of different scores.

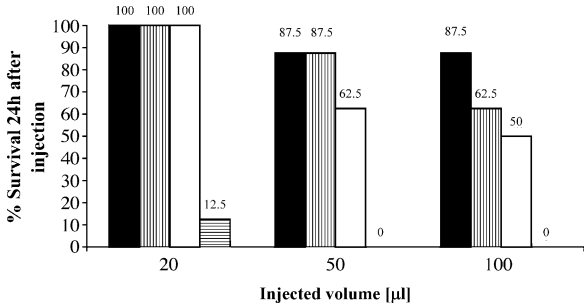

Fig. 2. Chick embryo survival rate 24 h after injection of NaCl 0.9% w/v (■) and solvent systems containing 50% v/v of water, 30% v/v of PEG 400 and 20% v/v of either DMSO (□), ethanol (▥) or benzyl alcohol (▤) (n = 8).

and 50 μl. Consequently, the system containing ethanol was selected as a reference in the PDT assays. Pharmacokinetics and PDT experiments were performed with 10 μl of this formulation.

4.2. Pharmacokinetic studies of p-THPP formulations

Pharmacokinetics and PDT experiments were conducted after IV administration of either *p*-THPP-loaded nanoparticles resuspended in PBS (*p*-THPP nanoparticles) or *p*-THPP dissolved in the ethanol system (free *p*-THPP). The pharmacokinetic profile of *p*-THPP following IV administration was determined by recording the fluorescence-time profiles of the drug. As shown in Fig. 3a and b, five seconds after infusion of both *p*-THPP formulations, the intravascular fluorescence intensity was high, as compared to the extravascular areas, indicating that the porphyrin was already distributed throughout the entire vascular system. However, *p*-THPP nanoparticles remained intravascular for at least 1500 s while free *p*-THPP had already leaked out from vascular system (Fig. 3c and d, respectively).

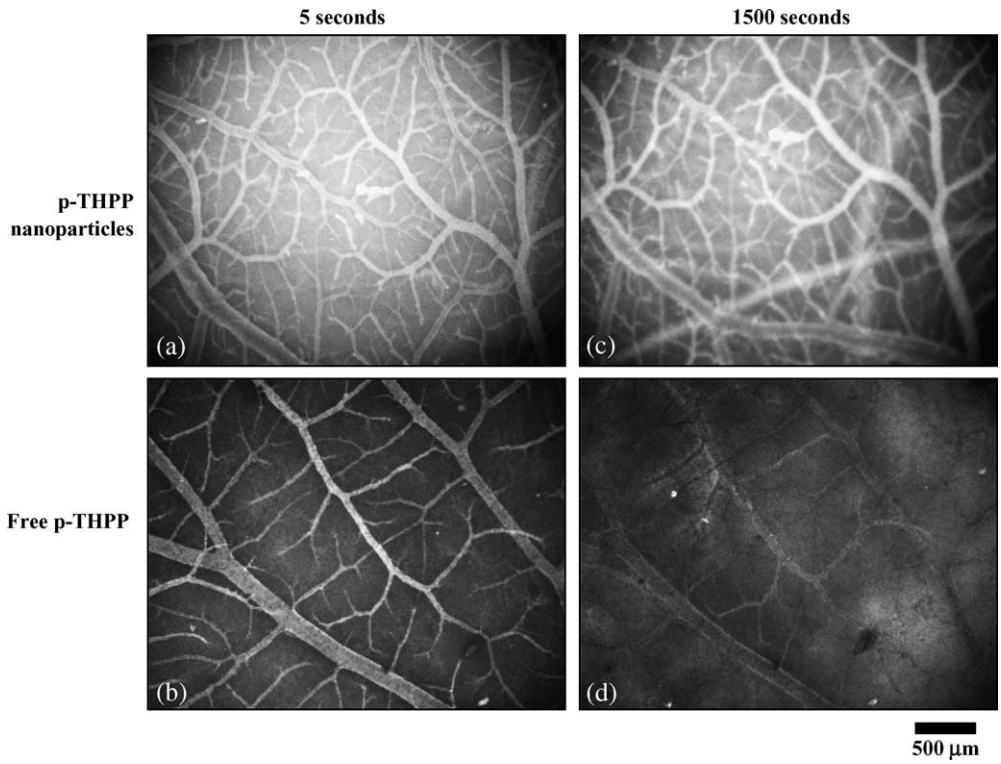

Fig. 3. Fluorescence angiographies ($\lambda_{excitation}$ = 400–440 nm and $\lambda_{emission}$ > 610 nm) of the CAM after administration of 0.6 mg of *p*-THPP per kg of chick embryo body weight. Upper panel: *p*-THPP loaded nanoparticles. Lower panel: free *p*-THPP (dissolved in a mixture of ethanol, PEG 400, and water 2:3:5 v/v/v). Pictures a and b were taken 5 s after administration, pictures c and d after 1500 s.

The calculation of the normalized photographic contrast from these fluorescence images at different times following injection allowed an indirect evaluation of the extent to which the photosensitizer diffused out from CAM vasculature (Fig. 4). High contrast values indicate that a small amount of the porphyrin leaked out from blood vessels. In contrast, when fluorescence values of *p*-THPP inside and outside CAM vasculature are similar, contrast diminishes, indicating the diffusion of *p*-THPP through the vessels. Fig. 4 clearly demonstrates the rapid extravasation of free *p*-THPP, while *p*-THPP nanoparticles remained longer in the intravascular compartment.

4.3. Influence of ethanol concentration on p-THPP extravasation

In order to evaluate the impact of the ethanol concentration on the leakage of *p*-THPP from CAM vasculature, we administered several formulations containing equivalent amounts of *p*-THPP (0.6 mg/ml) but

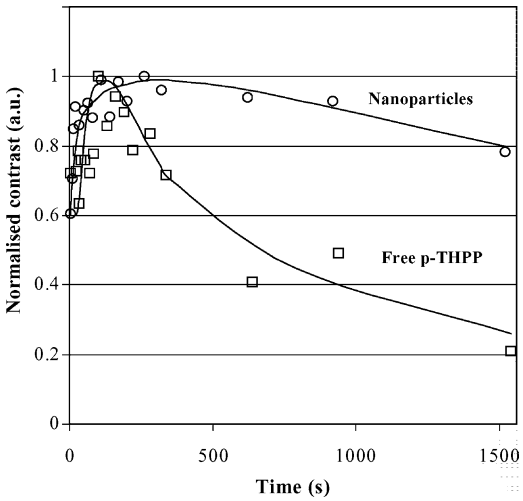

Fig. 4. Comparative pharmacokinetics of two *p*-THPP formulations. Evolution of fluorescence normalized contrast as a function of time after administration of *p*-THPP-loaded nanoparticles (◯) or free *p*-THPP (□). Dose of porphyrin: 0.6 mg per kg of chick embryo body weight. Normalized average (n = 3).

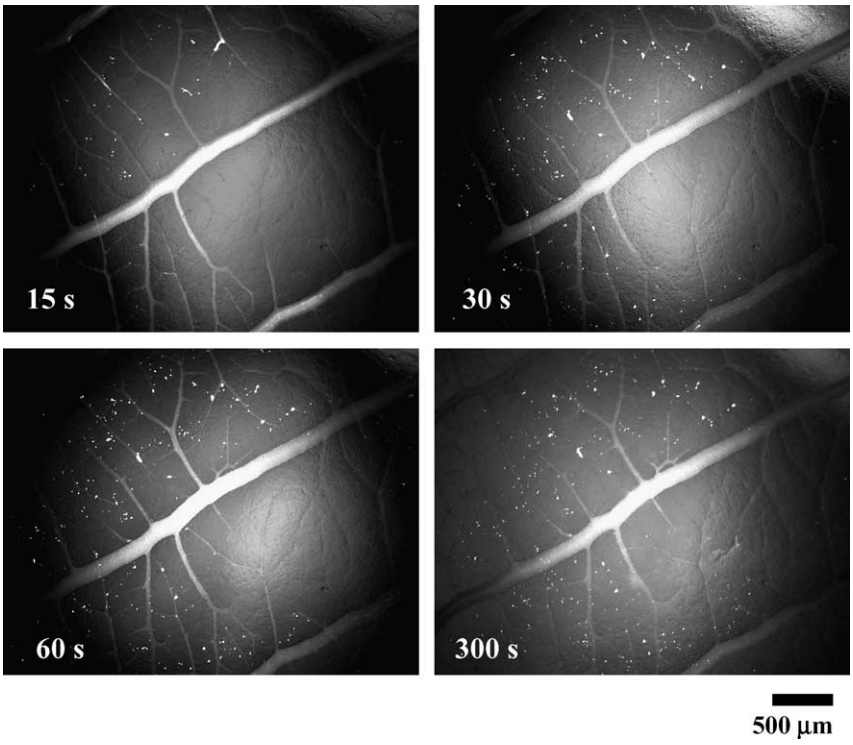

Fig. 5. Fluorescence angiographies ($\lambda_{excitation}$ = 400–440 nm and $\lambda_{emission}$ > 610 nm) after administration of 0.6 mg of *p*-THPP per kg of chick embryo body weight. Porphyrin was dissolved in 70% v/v of ethanol and 30% v/v of PEG 400.

increasing concentrations of ethanol (15, 20, 30, 40 or 70% v/v). PEG 400 concentration was kept constant at 30% v/v in all formulations. Fig. 5 shows a sequence of angiographies taken after administration of 10 μl of the formulation containing 70% v/v of ethanol. Localized spots of high fluorescence intensity were observed 15 s after administration. The number of these fluorescent dots increased until approximately 60 s, after which no changes appeared in the subsequent 240 s. The same effect was observed in other areas of the same egg (data not shown) and has been shown to be reproducible within these experiments. Fig. 6 shows a series of fluorescence angiographies corresponding to formulations containing 15, 20, 30, and 40% v/v of ethanol, taken 60 s after injection. From these experiments, it can be shown that the appearance of localized spots of high fluorescence occurs at ethanol concentrations above 20% v/v in the formulation.

4.4. Comparison of photodynamic activity of free and encapsulated p-THPP

A typical sequence of a CAM assay consisting of an injection of *p*-THPP formulation, followed by a photodynamic treatment and a sulforhodamine 101 angiography 24 h post-PDT is shown in Fig. 7. Since irradiation was performed on a reduced CAM surface (3 mm^2), direct comparison between irradiated and non-irradiated areas was possible. The PDT effect in this experiment was scored as 3 (see scale of damage in Table 1). As shown in Fig. 8, the photodynamic activity of the porphyrin increased with both light and *p*-THPP doses for both formulations. The damage induced on the vascular system varied from 0 to 5 and it was shown to be controlled by the variation of the *p*-THPP dose and irradiation conditions as established by PLUM ordinal regression statistical analysis. The differences between the two formulations were analysed using the

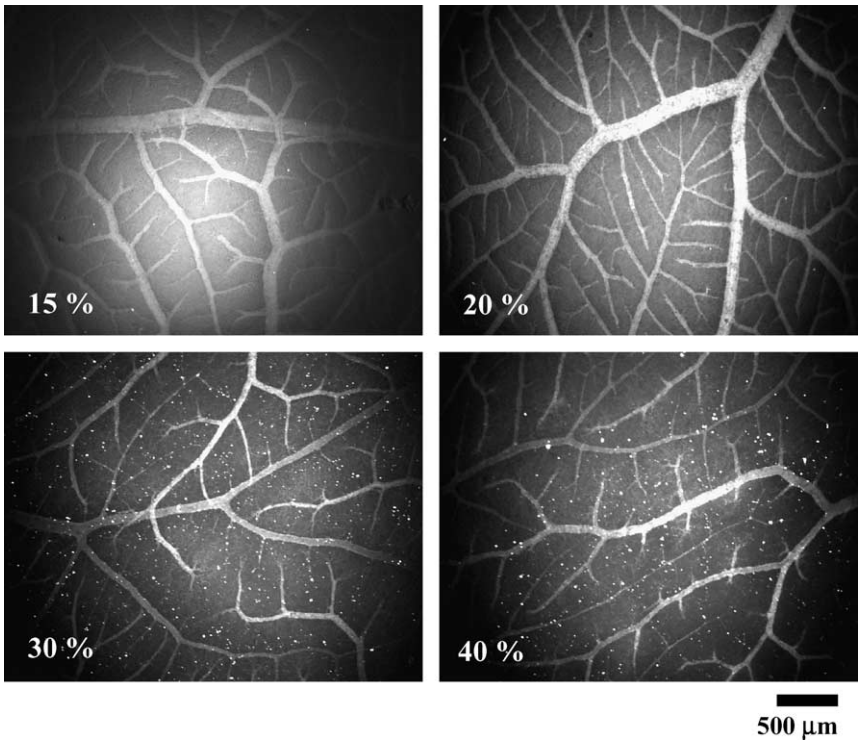

Fig. 6. Effect of ethanol concentration on *p*-THPP extravasation. Fluorescence angiographies ($\lambda_{excitation}$ = 400–440 nm and $\lambda_{emission}$ > 610 nm) were taken 60 s after administration of *p*-THPP formulations containing different concentrations of ethanol (% v/v is indicated in pictures). All formulations additionally contained 30% of PEG 400 and water q.s. Dose of *p*-THPP: 0.6 mg per kg of chick embryo body weight.

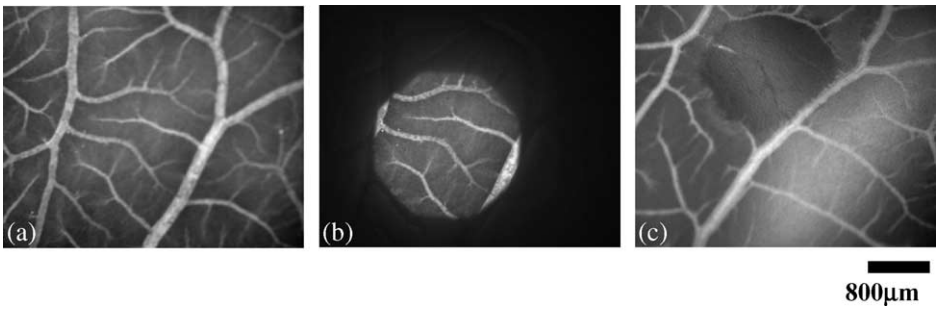

Fig. 7. Typical sequence of CAM assay: (a) administration of polymeric nanoparticles (1.2 mg of *p*-THPP per kg of embryo body weight); (b) irradiation with light dose of 15 J/cm^2. (c) angiography after sulforhodamine 101 injection, 24 h post PDT. The vascular damage was scored as 3 for this experiment (see Table 1). (a and b) $\lambda_{excitation}$ = 400–440 nm and $\lambda_{emission}$ > 610 nm. (c) $\lambda_{excitation}$ = 510–560 nm and $\lambda_{emission}$ > 590 nm.

Mann–Whitney test and a two-sided *P*-value less than 0.05 was considered significant. Across all evaluated conditions the phototoxic effects were statiscally significantly enhanced by the incorporation of *p*-THPP into PLGA nanoparticles as compared to free *p*-THPP (two-sided *P*-value = 0.024, size of population = 72 embryos, Mann–Whitney test). It is worth noting that under all conditions used, the apparent structure as well as the diameter of non-irradiated blood vessels remained unchanged.

5. Discussion

5.1. Development of an injectable soluble formulation of p-THPP

Since *p*-THPP is a very hydrophobic molecule that cannot be intravenously administered as a simple aqueous solution, cosolvents are needed to inject this compound for photodynamic purposes. Three different formulations using water and organic cosolvents (50% v/v of water, 30% v/v of PEG 400, and 20% v/v of either ethanol, DMSO or benzyl alcohol) were tested in this study. Polyethylene glycols (PEG 200 to PEG 600) are low toxicity compounds used as solvents for IV formulations (Mottu et al., 2000). PEG 400 is, indeed, accepted by the U.S. Food and Drug Administration for intramuscular and IV injection. Ethanol is a solvent for various drugs used in injectable formulations. DMSO is one of the most common solvents for the administration of several water-insoluble substances, although its use is controversial due to its local and hemodynamic toxicities (Santos et al., 2003). Benzyl alcohol is a bacteriostatic agent found in many parenteral formulations. In the present study, the concentration of ethanol, DMSO and benzyl alcohol was limited to 20% v/v in order to improve their blood compatibility (Montaguti et al., 1994). Since the three formulations contained 50% v/v of water, we were interested in the evaluation of the aggregation of *p*-THPP in such environments. Aggregation is relevant in PDT, because aggregated PS are expected to be less efficient as sensitizers than the monomeric species (Isele et al., 1994; Ricchelli, 1995; Bonnett et al., 2001). Electronic spectroscopy is one of the experimental methods used for detecting this phenomenon. For example, aggregation of meta-tetra(*m*-hydroxyphenyl) chlorin (*m*-THPC) in aqueous solutions containing methanol has been characterized by a broadening of the Soret band, a red shift of λ_{max} (wavelength of maximal absorption) and a decrease of ε_{max} (molar extinction coefficient at λ_{max}) (Bonnett et al., 2001). The spectral data for the three formulations (Fig. 1b) show the typical Soret band at around 425 nm and several weaker absorptions (Q bands) at higher wavelengths. These characteristic bands are typical for porphyrins indicating the absence of aggregation. In our study, the tolerability and safety of the solvents were tested prior to investigations of the PDT efficacy. Only the solvent system containing ethanol showed an acceptable tolerance by chick embryos on EDD 12 with survival rates similar to those obtained with NaCl aqueous solution (Fig. 2). Toxicity of the DMSO-containing formulation can be associated with the haemolytic activity of DMSO (Mottu et al., 2001). In agreement with our results, Gottfried

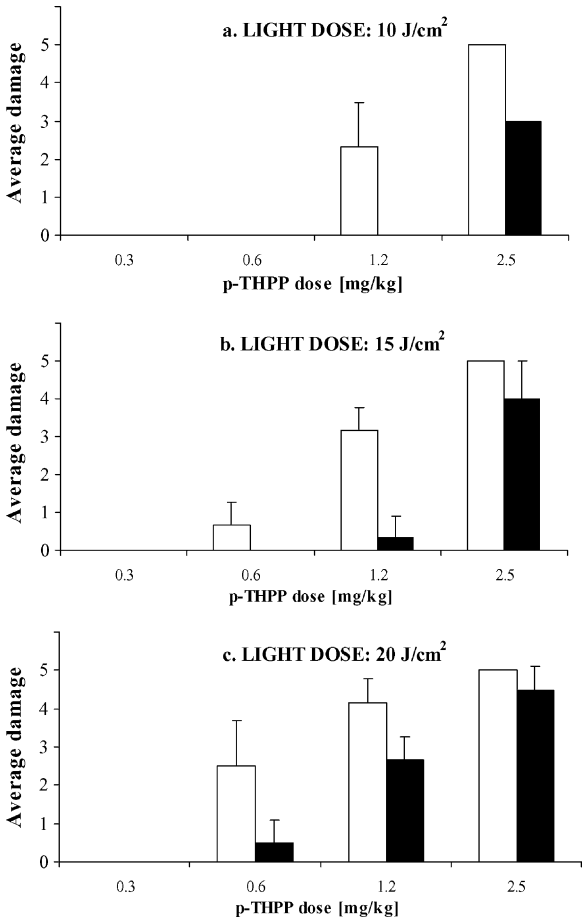

Fig. 8. Comparison of the vascular damage induced by *p*-THPP-loaded nanoparticles (□) and *p*-THPP solution (■) in ethanol, PEG 400, and water 2:3:5 v/v/v. CAM was irradiated with various light doses: (a) 10 J/cm^2; (b) 15 J/cm^2; and (c) 20 J/cm^2. Mean + S.D. (n = 3). Columns showing no bars indicate that the S.D. values for those conditions were zero. Statistical analysis of the overall results demonstrate that nanoparticles induced a higher photodynamic effect than solution did, across the different light and *p*-THPP doses (two-sided *P*-value = 0.024, size of population = 72 embryos, Mann–Whitney test).

et al. (1995) found 10% v/v DMSO in water to be toxic to 10-day-old chick embryos. In our model, the formulation containing benzyl alcohol was the most toxic. Interestingly, it has been previously reported that the toxicity of benzyl alcohol in neonatal mice can be presumably attributed to its metabolite, benzoic acid (McCloskey et al., 1986). Indeed, the process of detoxification of benzyl alcohol appeared to be inefficient in human premature neonates (LeBel et al., 1988). The solvent system selected to administer *p*-THPP to embryos containing ethanol, PEG 400 and water at 2:3:5 v/v/v has been previously used to dissolve *m*-THPC during in vivo PDT assays in mice (Westerman et al., 1998) and hamster cancer models (Glanzmann et al., 2000). It is worth noting that the injected volume was critical regardless of the type of solvent used (Fig. 2). In the literature, the reported volume of liquids administered to chick embryos is variable: 10 μl for embryos on EDD 3 and 4 (total blood volume 50 and 100 μl) (Hu et al., 1996), 100 μl for embryos on EDD 12 (total blood volume approximately 1.6 ml) (Lange et al., 2001), and 200 μl for embryos on EDD 10 and 19 (total blood volume 1 and 3 ml, respectively) (Mulder et al., 1997). The values of total blood volume of chick's embryos were taken from Romanoff (1967). In view of the results of the tolerance experiments (Fig. 2) a volume of 10 μl was chosen for further experiments.

5.2. Pharmacokinetics, extravasation and photodynamic activity of p-THPP

This study showed: (i) *p*-THPP remained longer in the vascular compartment when incorporated into nanoparticles and (ii) vascular occlusion after PDT was enhanced when using nanoparticle carriers as compared to a *p*-THPP solution.

The pharmacokinetics of *p*-THPP (Fig. 4) were evaluated on the CAM model by measuring the variations of the fluorescence intensity of this molecule inside and outside vessels as a function of time. These changes may be attributed to (i) a change in the fluorescence properties of circulating *p*-THPP after aggregation or disaggregation, binding to vasculature walls or interaction with blood components, such as lipoproteins or (ii) a modification of the concentration of the *p*-THPP present in the different compartments; the disappearance of *p*-THPP from the intravascular system might be associated with porphyrin metabolism, plasmatic clearance, capture of the drug carrier by the phagocytic system and extravasation from vessels. However, under the conditions of this study, the CAM assay does not allow us to discriminate between these hypotheses. Partitioning of photosensitizer between vasculature and adjacent tissues will be of particular interest in cases where PDT leads to unwanted therapeutic effects in extravascular compartments. For example, during the photodynamic treatment of CNV associated with AMD, the

Table 2
The principal factors controlling the extravasation of molecules (Takakura et al., 1998; Desmettre et al., 2000)

Biological factors	Physicochemical properties of both the drug and the carrier
Regional differences in the capillary structures	Molecular size
Disease state of the organ or tissue	Shape
Rate of blood and lymph supply	Charge
	Hydrophilic/lipophilic balance (HLB)
	Properties of surface

photosensitizing agent should not significantly leak out of the fenestrated neovessels in order to prevent photodynamic damage of neighbouring structures such as the retinal pigment epithelium or the photoreceptors. These undesired effects are particularly problematic when retreatment is necessary, due to the incomplete occlusion of CNV (Renno and Miller, 2001; Moshfeghi et al., 2003).

Molecules can extravasate across the normal endothelium by transcapillary pinocytosis as well as by passage through interendothelial cell junctions, gaps or fenestrae (Takakura et al., 1998). The diffusion of a molecule through biological barriers, such as the endothelial walls, depends both on the physicochemical properties of the molecule and on the structure of the barrier itself (see Table 2).

Molecular weight has been shown to be a critical factor for endothelial permeability. Conjugation of low molecular weight drugs, which freely diffuse throughout the body, to macromolecular carriers ($M_r \geq 70{,}000$) restricts their extravasation (Takakura et al., 1998). Indeed, several studies on in vivo cancer models have shown the way in which the size of both the drug and the carrier are critical for extravasation of angiogenesis contrast agents (Weissleder et al., 2001) or PEG-coated liposomes (Ishida et al., 1999). Consequently, entrapment of *p*-THPP (M_w: 679 g/mol) into 117 nm PLGA-nanoparticles led to an increase of the intravascular residence time as compared to free *p*-THPP in solution. As solid polymeric aggregates, particles cannot cross the vascular endothelium unless it is itself leaky (Moghimi et al., 2001), therefore, they are expected to remain within the vascular compartment until they are degraded or otherwise eliminated. Furthermore, due to their rigidity, nanoparticles could have advantages over liposomes. It has been shown that the clearance of liposomes as well as the encapsulated drug is significantly dominated by the fluidity and the nature of the liposomal bilayer (Drummond et al., 1999). Romero et al. (1999) showed that highly deformable vesicles of up to 400 nm can reach the hepatic sinusoidal endothelium although size fenestrations range between 100 and 150 nm. The authors suggested that the liposomes are forcefully squeezed or extruded through the fenestrations, mediated by a process of forced sieving involving blood cells. Such a passage involves the deformation of the liposomal bilayer to adjust to the much smaller size of the fenestrae (Romero et al., 1999). On the other hand, Woodle (1998) demonstrated that a prolonged circulation of liposomes can be achieved when increasing the cohesive nature of the bilayer. Hence, the deformability of the drug carrier becomes an important property directing the extravasation of drugs.

The enhanced PDT effect of *p*-THPP nanoparticles might be associated not only with the increased residence time inside the vascular bed but also with the localization of nanoparticles within the vascular wall itself. Accordingly, studies performed in ex vivo models demonstrated that nanoparticles (30–500 nm) are taken up by the arterial wall of canine carotid artery (Song et al., 1997) and pig coronary artery (Labhasetwar et al., 1998). However, as the mechanisms which result in the penetration and retention of nanoparticles in endothelial cells are incompletely understood, microscopy and histological studies should be developed to test this hypothesis.

The impact of the liposolubility of a fluorescent dye on its extravasation has been studied in rabbits and primates with fluorescein and two of its derivatives (Fang et al., 1990); a higher liposolubility was found to reduce extravasation from choroidal vasculature. Despite the hydrophobic character of *p*-THPP, its extravasation was high when it was in solution, formulated in ethanol, PEG 400 and water (2:3:5 v/v/v). Therefore, it was interesting to evaluate whether ethanol would influence the extravasation of *p*-THPP. The concentration of ethanol in the formulation was dictated by the solubility of *p*-THPP. To dissolve *p*-THPP at the

highest concentration used in this study (2.5 mg/ml, for a *p*-THPP dose of 2.5 mg per kg of embryo) it was necessary to use at least 20% v/v of ethanol in the formulation.

The effect of the ethanol concentration on the extravasation of *p*-THPP was tested with formulations containing 15, 20, 30, 40 and 70% v/v of this solvent. The results of these studies suggested a relationship between the concentration of ethanol present in the formulation and the appearance of highly fluorescent spots (Figs. 5 and 6). This phenomenon can presumably be attributed to either the interaction of ethanol with blood components or the effect of this solvent on the integrity of the vasculature walls, which could result in the extravasation of the photosensitizer. Ethanol has been shown to cause concentration-dependent aggregation of platelets in whole blood of human and rats (Abi-Younes et al., 1991). Furthermore, high intravascular concentrations of ethanol have been reported to alter the conformation and stability of human serum albumin and haemoglobin (Ostrovsky et al., 1987) and induce conformational changes of human low density plasma lipoproteins (Kveder et al., 1997). In the context of PDT, these phenomena might be of major importance since hydrophobic photosensitizers have been shown to be associated with lipoproteins following IV administration (Allison et al., 1994; Reddi, 1997; Schmidt-Erfurth and Hasan, 2000). We hypothesize that the administration of formulations containing high concentrations of ethanol induced the aggregation of *p*-THPP blood carriers leading to the formation of high fluorescent spots observed on the angiographies of CAM (Figs. 5 and 6). On the other hand, the appearance of those fluorescent spots could also be related to ethanol-induced damage of the endothelial tissues, which can favour the extravascular localisation of those fluorescent aggregates. Sampei et al. (1996) have investigated the extravasation of Evans blue into rat brain tissue after administering aqueous solutions containing increasing concentrations of ethanol. They found that this effect was dependent on the ethanol concentration, its total dose, the duration of the exposure to the endothelium and the actual concentration of the solvent at the surface of the endothelium. Indeed, high concentrations of ethanol (40–70%) have been reported to induce necrosis of the full thickness of the vessels wall and swelling of brain cells (Sampei et al., 1996). Another histological study revealed extensive endothelial damage and sloughing following intraarterial injection of absolute ethanol in dogs (Ellman et al., 1984). Further experiments should be carried out in order to explain the underlying mechanisms of the formation of the high fluorescent spots observed on the angiographies of CAM (Figs. 5 and 6).

This evidence highlights the importance of the development of adequate PS carriers. Thus, even if solvents used in drug formulations are well tolerated by patients, they might alter the integrity of the vasculature or the drug carriers (such as lipoproteins, in the case of PS transport in bloodstream), altering the biodistribution and thereby hampering the targeting and the controlled delivery of drugs.

As mentioned above, the magnitude of the extravasation of molecules will ultimately be determined by the physicochemical properties of both the drug and its carrier. However, it is relevant to discuss some additional issues particularly associated with PDT. Increase in vascular permeability and vessel constriction are part of the vascular effects of PDT (Fingar, 1996; Krammer, 2001). Indeed, changes in the CAM microcirculation and blood vessel morphology have been observed during PDT when using porphycenes incorporated into liposomes (Gottfried et al., 1995). Differences in PDT efficacy of both *p*-THPP formulations used in our study could also be a consequence of the photodynamic treatment itself. If an increase of vascular permeability is produced during PDT, nanoparticles might be less likely to extravasate vessels than free porphyrin, leading to an enhanced PDT effect when using the nanocarrier. Actually, the dose of the photosensitizer needed to achieve a similar effect can be reduced by incorporation into nanoparticles (Fig. 8). Consequently, the use of nanoparticles could result in a localized PDT effect on vessels, where the photodynamic destruction of adjacent tissues could be avoided.

6. Conclusion

We have demonstrated that PDT-induced vascular occlusion of the photosensitizer *p*-THPP is enhanced when encapsulated into nanoparticle delivery systems. The superiority of nanoparticles over solubilized *p*-THPP might be related to the reduced diffusion of *p*-THPP nanoparticles out of the vessels. Free *p*-THPP appeared to leak out before generating an efficient

vascular occlusion, whereas nanoparticles appear to confer a longer residence time inside the vasculature and may also interact differently with the vessel walls.

Since under the same irradiation conditions *p*-THPP nanoparticles induced an increased PDT effect, compared to free *p*-THPP, porphyrin doses can be diminished to achieve the desired therapeutic effect. Consequently, fewer side effects related to the diffusion of PS into surrounding tissues can be expected. Another advantage of the incorporation of *p*-THPP into polymeric nanocarriers is the possibility of administering intravenously a hydrophobic PS without the use of solvents, such as ethanol, which might react with endothelial tissues.

This study indicates that for achieving a selective destruction of vasculature (while protecting surrounding tissues), an increase in the residence time of the PS in blood vessels during light activation is mandatory. Therefore, the increased retention of nanoparticles inside vessels, which results in the possibility of diminishing the PS doses, might be useful to overcome the adverse effects seen during photodynamic treatment of CNV associated with AMD. Nevertheless, as it is not clear whether the CAM model can distinguish between proliferating and non-proliferating blood vessels (Lange et al., 2001; Ribatti et al., 2001), in vivo models exhibiting other biological and pathological structures of interest, should be developed to evaluate the performance of PS nanocarriers. Actually, since little is known about the circulation time of colloidal carriers in chick embryos, one should be careful with the direct extrapolation of the results found in the CAM model to other organisms.

Acknowledgments

The authors thank Professor Dr. Michael Eid (Department of Psychology, University of Geneva) for performing the statistical analysis of the experimental data.

References

Abi-Younes, S.A., Ayers, M.L., Myers, A.K., 1991. Mechanism of ethanol-induced aggregation in whole blood. Thromb. Res. 63, 481–489.

Allison, B.A., Pritchard, P.H., Levy, J.G., 1994. Evidence for low-density lipoprotein receptor-mediated uptake of benzoporphyrin derivative. Br. J. Cancer 69, 833–839.

Barnes, A.E., Jensen, W.N., 1959. Blood volume and red cell concentration in the normal chick embryo. Am. J. Physiol. 197, 403–405.

Bonnett, R., Djelal, B.D., Nguyen, A., 2001. Physical and chemical studies related to the development of m-THPC (FOSCAN®) for the photodynamic therapy (PDT) of tumors. J. Porphyrins Phthalocyanines 5, 652–661.

Derycke, A.S.L., de Witte, P.A.M., 2004. Liposomes for photodynamic therapy. Adv. Drug Deliv. Rev. 56, 17–30.

Desmettre, T., Devoisselle, J.M., Mordon, S., 2000. Fluorescence properties and metabolic features of indocyanine green (ICG) as related to angiography. Surv. Ophthalmol. 45, 15–27.

Dougherty, T.J., Gomer, C.J., Henderson, B.W., Jori, G., Kessel, D., Korbelik, M., Moan, J., Peng, Q., 1998. Photodynamic therapy. J. Natl. Cancer Inst. 90, 889–905.

Drummond, D.C., Meyer, O., Hong, K., Kirpotin, D.B., Papahadjopoulos, D., 1999. Optimizing liposomes for delivery of chemotherapeutic agents to solid tumors. Pharmacol. Rev. 51, 691–743.

Ellman, B.A., Parkhill, B.J., Marcus, P.B., Curry, T.S., Peters, P.C., 1984. Renal ablation with absolute ethanol. Mechanism of action. Invest. Radiol. 19, 416–423.

Fang, T., Naguib, K.S., Peyman, G.A., Khoobehi, B., 1990. Comparative study of three fluorescent dyes for angiography: sodium fluorescein, carboxyfluorescein, and calcein. Ophthalmic Surg. 21, 250–257.

Ferris III., F.L., Fine, S.L., Hyman, L., 1984. Age-related macular degeneration and blindness due to neovascular maculopathy. Arch. Ophthalmol. 102, 1640–1642.

Fingar, V.H., 1996. Vascular effects of photodynamic therapy. J. Clin. Laser Med. Surg. 14, 323–328.

Gelderblom, H., Verweij, J., Nooter, K., Sparreboom, A., 2001. Cremophor EL: the drawbacks and advantages of vehicle selection for drug formulation. Eur. J. Cancer 37, 1590–1598.

Glanzmann, T., Forrer, M., Blant, S.A., Woodtli, A., Grosjean, P., Braichotte, D., van den Bergh, H., Monnier, P., Wagnieres, G., 2000. Pharmacokinetics and pharmacodynamics of tetra(*m*-hydroxyphenyl)chlorin in the hamster cheek pouch tumor model: comparison with clinical measurements. J. Photochem. Photobiol. B 57, 22–32.

Gottfried, V., Davidi, R., Averbuj, C., Kimel, S., 1995. In vivo damage to chorioallantoic membrane blood vessels by porphycene-induced photodynamic therapy. J. Photochem. Photobiol. B 30, 115–121.

Hammer-Wilson, M.J., Akian, L., Espinoza, J., Kimel, S., Berns, M.W., 1999. Photodynamic parameters in the chick chorioallantoic membrane (CAM) bioassay for topically applied photosensitizers. J. Photochem. Photobiol. B 53, 44–52.

Hornung, R., Hammer-Wilson, M.J., Kimel, S., Liaw, L.H., Tadir, Y., Berns, M.W., 1999. Systemic application of photosensitizers in the chick chorioallantoic membrane (CAM) model: photodynamic response of CAM vessels and 5-aminolevulinic acid uptake kinetics by transplantable tumors. J. Photochem. Photobiol. B 49, 41–49.

Hu, N., Thang, D.N., Clark, E.B., 1996. Distribution of blood flow between embryo and vitelline bed in the stage 18, 21 and 24 chick embryo. Cardiovasc. Res. 31, E127–E131.

Isele, U., Schieweck, K., Kessler, R., van Hoogevest, P., Capraro, H.G., 1994. Pharmacokinetics and body distribution of liposomal zinc phthalocyanine in tumor-bearing mice: influence of aggregation state, particle size, and composition. J. Pharm. Sci. 84, 166–173.

Ishida, O., Maruyama, K., Sasaki, K., Iwatsuru, M., 1999. Size-dependent extravasation and interstitial localization of polyethyleneglycol liposomes in solid tumor-bearing mice. Int. J. Pharm. 190, 49–56.

Klein, R., Klein, B.E., Linton, K.L., 1992. Prevalence of age-related maculopathy. The Beaver Dam eye study. Opthalmology 99, 933–943.

Konan, Y.N., Cerny, R., Favet, J., Berton, M., Gurny, R., Allemann, E., 2003a. Preparation and characterization of sterile sub-200 nm meso-tetra(4-hydroxylphenyl)porphyrin-loaded nanoparticles for photodynamic therapy. Eur. J. Pharm. Biopharm. 55, 115–124.

Konan, Y.N., Berton, M., Gurny, R., Allemann, E., 2003b. Enhanced photodynamic activity of meso-tetra(4-hydroxyphenyl)porphyrin by incorporation into sub-200 nm nanoparticles. Eur. J. Pharm. Sci. 18, 241–249.

Konan, Y.N., Gurny, R., Allemann, E., 2002. State of the art in the delivery of photosensitizers for photodynamic therapy. J. Photochem. Photobiol. B 66, 89–106.

Krammer, B., 2001. Vascular effects of photodynamic therapy. Anticancer Res. 21, 4271–4277.

Kveder, M., Pifat, G., Pecar, S., Schara, M., Ramos, P., Esterbauer, H., 1997. The interaction of lower alcohols with apoB in spin labeled human plasma low density lipoproteins (LDL). Chem. Phys. Lipids 87, 125–135.

Labhasetwar, V., Song, C., Humphrey, W., Shebuski, R., Levy, R.J., 1998. Arterial uptake of biodegradable nanoparticles: effect of surface modifications. J. Pharm. Sci. 87, 1229–1234.

Lange, N., Ballini, J.P., Wagnieres, G., van den Bergh, H., 2001. A new drug-screening procedure for photosensitizing agents used in photodynamic therapy for CNV. Invest. Ophthalmol. Vis. Sci. 42, 38–46.

LeBel, M., Ferron, L., Masson, M., Pichette, J., Carrier, C., 1988. Benzyl alcohol metabolism and elimination in neonates. Dev. Pharmacol. Ther. 11, 347–356.

Leroux, J.C., Allemann, E., De Jaeghere, F., Doelker, E., Gurny, R., 1996. Biodegradable nanoparticles from sustained release formulations to improved site specific drug delivery. J. Control. Rel. 39, 339–350.

McCloskey, S.E., Gershanik, J.J., Lertora, J.J.L., White, L., George, W.J., 1986. Toxicity of benzyl alcohol in adult and neonatal mice. J. Pharm. Sci. 75, 702–705.

Moghimi, S.M., Hunter, A.C., Murray, J.C., 2001. Long-circulating and target-specific nanoparticles: theory to practice. Pharmacol. Rev. 53, 283–318.

Montaguti, P., Melloni, E., Cavalletti, E., 1994. Acute intravenous toxicity of dimethyl sulfoxide, polyethylene glycol 400, dimethylformamide, absolute ethanol, and benzyl alcohol in inbred mouse strains. Arzneimittelforschung 44, 566–570.

Moshfeghi, D.M., Kaiser, P.K., Grossniklaus, H.E., Sternberg Jr., P., Sears, J.E., Johnson, M.W., Ratliff, N., Branco, A., Blumenkranz, M.S., Lewis, H., 2003. Clinicopathologic study after submacular removal of choroidal neovascular membranes treated with verteporfin ocular photodynamic therapy. Am. J. Ophthalmol. 135, 343–350.

Mottu, F., Laurent, A., Rufenacht, D.A., Doelker, E., 2000. Organic solvents for pharmaceutical parenterals and embolic liquids: a review of toxicity data. PDA J. Pharm. Sci. Technol. 54, 456–469.

Mottu, F., Stelling, M.J., Rufenacht, D.A., Doelker, E., 2001. Comparative hemolytic activity of undiluted organic water-miscible solvents for intravenous and intra-arterial injection. PDA J. Pharm. Sci. Technol. 55, 16–23.

Mulder, T.L.M., van Golde, J.C., Prinzen, F.W., Blanco, C.E., 1997. Cardiac output distribution in the chick embryo from stage 36 to 45. Cardiovasc. Res. 34, 525–528.

Ostrovsky, Yu.M., Stepuro, I.I., Artsukevich, A.N., Zavodnik, I.B., Konovalova, N.V., Lapshina, E.A., 1987. Interaction of ethanol with blood proteins. Alcohol Alcohol., 283–287.

Peterka, M., Klepacek, I., 2001. Light irradiation increases embryotoxicity of photodynamic therapy sensitizers (5-aminolevulinic acid and protoporphyrin IX) in chick embryos. Reprod. Toxicol. 15, 111–116.

Reddi, E., 1997. Role of delivery vehicles for photosensitizers in the photodynamic therapy of tumours. J. Photochem. Photobiol. B 37, 189–195.

Renno, R.Z., Miller, J.W., 2001. Photosensitizer delivery for photodynamic therapy of choroidal neovascularization. Adv. Drug Deliv. Rev. 52, 63–78.

Ribatti, D., Nico, B., Vacca, A., Roncali, L., Burri, P.H., Djonov, V., 2001. Chorioallantoic membrane capillary bed: a useful target for studying angiogenesis and anti-angiogenesis in vivo. Anat. Rec. 264, 317–324.

Ricchelli, F., 1995. Photophysical properties of porphyrins in biological membranes. J. Photochem. Photobiol. B 29, 109–118.

Romanoff, A.L., 1967. Biochemistry of the avian embryo: a quantitative analysis of prenatal development. John Wiley & Sons, New York.

Romero, E.L., Morilla, M.J., Regts, J., Koning, G.A., Scherphof, G.L., 1999. On the mechanism of hepatic transendothelial passage of large liposomes. FEBS Lett. 448, 193–196.

Sampei, K., Hashimoto, N., Kazekawa, K., Tsukahara, T., Iwata, H., Takaichi, S., 1996. Histological changes in brain tissue and vasculature after intracarotid infusion of organic solvents in rats. Neuroradiology 38, 291–294.

Santos, N.C., Figueira-Coelho, J., Martins-Silva, J., Saldanha, C., 2003. Multidisciplinary utilization of dimethyl sulfoxide: pharmacological, cellular, and molecular aspects. Biochem. Pharmacol. 65, 1035–1041.

Schmidt-Erfurth, U., Hasan, T., 2000. Mechanisms of action of photodynamic therapy with verteporfin for the treatment of age-related macular degeneration. Surv. Ophthalmol. 45, 195–214.

Sharman, W.M., Allen, C.M., van Lier, J.E., 1999. Photodynamic therapeutics: basic principles and clinical applications. Drug Discov. Today 4, 507–517.

Song, C.X., Labhasetwar, V., Murphy, H., Qu, X., Humphrey, W.R., Shebuski, R.J., Levy, R.J., 1997. Formulation and

characterization of biodegradable nanoparticles for intravascular local drug delivery. J. Control. Rel. 43, 197–212.
Sternberg, E.D., Dolphin, D., Bruckner, C., 1998. Porphyrin-based photosensitizers for use in photodynamic therapy. Tetrahedron 54, 4151–4202.
Takakura, Y., Mahato, R.I., Hashida, M., 1998. Extravasation of macromolecules. Adv. Drug Deliv. Rev. 34, 93–108.
Toledano, H., Edrei, R., Kimel, S., 1998. Photodynamic damage by liposome-bound porphycenes: comparison between in vitro and in vivo models. J. Photochem. Photobiol. B 42, 20–27.
Weissleder, R., Bogdanov Jr., A., Tung, C.H., Weinmann, H.J., 2001. Size optimization of synthetic graft copolymers for in vivo angiogenesis imaging. Bioconjug. Chem. 12, 213–219.
Westerman, P., Glanzmann, T., Andrejevic, S., Braichotte, D.R., Forrer, M., Wagnieres, G.A., Monnier, P., van den Bergh, H., Mach, J.P., Folli, S., 1998. Long circulating half-life and high tumor selectivity of the photosensitizer meta-tetrahydroxyphenylchlorin conjugated to polyethylene glycol in nude mice grafted with a human colon carcinoma. Int. J. Cancer 76, 842–850.
Woodle, M.C., 1998. Controlling liposome blood clearance by surface-grafted polymers. Adv. Drug Deliv. Rev. 32, 139–152.